

Estimation of Time-Varying Inertia of Aerial Manipulators Performing Manipulation of Unknown Objects

Chanhong Park, Alejandro Ramirez-Serrano, Mahdis Bisheban

University of Calgary
Calgary, Alberta, Canada

chanhong.park1@ucalgary.ca; aramirez@ucalgary.ca; mahdis.bisheban@ucalgary.ca

Abstract – This paper presents a method for estimating the varying inertia parameters of unmanned aerial manipulators (UAMs) while they perform manipulation maneuvers on a priori unknown objects and execute various flight maneuvers. The varying mass and moment of inertia tensor of the UAM are estimated using the UAM's force and the kinematic model of its robotic arm by means of a novel sequential Kalman filter (KF) algorithm. In order to validate the effectiveness of the mechanism, it is implemented on a highly-maneuverable VTOL-type UAV equipped with a 3 degree-of-freedom (DoF) manipulator capable of moving only on the longitudinal plane of the aircraft.

Keywords: Unmanned aerial manipulator, Kalman filter, parameter estimation, varying inertia parameters.

1. Introduction

Over the past few decades, unmanned aerial vehicles (UAVs) have garnered increasing attention for their use in military and civilian applications. To further enhance the capabilities of UAVs, researchers have been working on combining robotic arms with UAVs, creating what are known as unmanned aerial manipulators (UAMs) [1-2].

Controlling UAMs for complex missions that require simultaneous arm manipulation while performing flight maneuvers has been a challenging task that requires further attention. Controlling the arm motion while the UAV is stationary (i.e., hovering) has been the traditional approach used in UAM control [3-4]. Performing manipulation under such conditions, however, is limited and does not maximize the capabilities of UAMs. As a result, current UAMs are incapable of performing diverse tasks that are needed, such as dynamically capturing objects while maintaining translational motions or using the arm as an agent to enhance the flying capabilities of the UAV (e.g., flight maneuvers that eagles perform with captured prey in nature). One of the main factors that make the control of UAMs challenging is the varying inertia parameters, such as changes in the total mass of the UAV, moments of inertia, and variations in the UAV's center of mass. Control performance heavily depends on the accuracy of the model parameters used in the UAM's mathematical model, including drag coefficient changes and, more importantly, inertia parameters. However, even small manipulation maneuvers performed by the UAM cause these inertia parameters to change. These changes are typically more pronounced when grasping and manipulating a priori unknown mass objects. For example, when a given UAM picks up an object, all of its inertia parameters and dynamics are altered. Similarly, changes in the arm's position and (unknown) deflection of its linkages can result in changes to the moment of inertia and the center of mass of the UAM. These changes can significantly degrade control performance or disrupt the UAV's flight maneuvers. Therefore, it is necessary to develop real-time estimation algorithms to handle changes in inertia parameters in order to maintain the stability and maneuverability of UAMs at all times during a given mission.

There have been numerous research papers dealing with varying inertia parameters for aerial vehicles. The most commonly used methods to cope with this problem has been the use of adaptive laws [5-6]. In [7], Min et al. utilized an adaptive robust controller to estimate the mass of UAVs that carry unknown payloads to achieve effective altitude control. Baraban et al. [8] designed a model reference adaptive law to estimate the varying mass of UAMs during pick-up maneuvers using acceleration measurement and low-pass filters. These and other approaches typically take several seconds for estimation variables to converge, which is not suitable for real-time control purposes during critical flight maneuvers. In [9-10], Lee and Kim suggested the use of an online parameter estimator for unknown payloads picked up using Lyapunov candidate functions. Mellinger et al. in [11] used recursive least square methods for mass, center of mass, and lateral aerodynamic disturbance estimation through a set of independent online estimation algorithms. Although practical and

somewhat generic, the approach proposed in [11] requires that the UAV be in a stable and controllable hover flight when the presence of varying parameters exists.

Although previous research works have been effective, they did not consider the highly nonlinear kinematics and dynamics of the manipulator, which are closely related to changes in the inertia parameters of the UAM. In this paper, a cascade Kalman Filter (KF) mechanism [12] is proposed to control a novel highly maneuverable Vertical Take-Off and Landing (VTOL) UAV with a 3-DoF robotic arm developed for operations inside confined spaces [13]. The proposed mechanism leverages the UAV dynamics and the 3-DoF manipulator kinematics to enhance the UAV's flight characteristics.

The remainder of this paper is organized as follows. Section 2 describes the UAM used in this research work. Section 3 presents the procedure of estimation for the mass and moment of inertia tensor of the UAM. Section 4 provides simulation results and finally, the conclusions are given in Section 5.

2. The UAM

The UAM of interest is a VTOL-type UAV named Navig8. It has the unique ability to perform flight maneuvers that other aircraft cannot execute, such as pitch hovering at any angle within the range of -90° to $+90^\circ$ (Fig. 1-(a)) [13-15]. This UAV has been equipped with a 3-DoF manipulator that can only move within the longitudinal plane of the aircraft, as shown in Fig. 1-(b) and Fig. 1-(c). The joints of the arm are all revolute, with axes of the rotation parallel to each other (Fig. 3). The UAV component of the UAM is controlled by two tilting ducted variable-pitch propellers and one variable-pitch horizontal tail propeller. The two main propellers are independently tiltable in the longitudinal direction to produce thrust vectoring forces, as illustrated in Fig. 1-(c), where the left and right propellers are tilted forward and backwards, respectively.

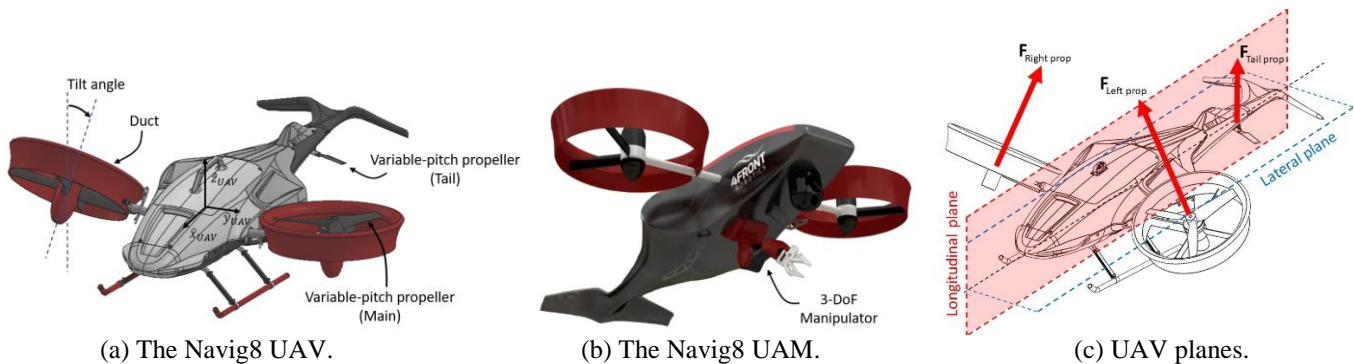


Fig. 1: The Navig8 UAV and hypothetical Navig8 UAM.

3. Estimation Filter Design

The proposed estimation algorithm comprises two intertwined Kalman Filters to estimate the mass including any mass grabbed by the arm and moments of inertia of the UAM, as schematically illustrated in Fig. 2. The first Kalman filter utilizes measurements of the propellers' angular velocities ($\vec{\omega}_{prop}$), the UAV's linear acceleration (\vec{a}_{UAV}), and its angular velocity ($\vec{\omega}_{UAV} = [P, Q, R]^T_{UAV}$) and acceleration ($\vec{\alpha}_{UAV} = [\dot{P}, \dot{Q}, \dot{R}]^T_{UAV}$) to estimate the UAM's mass. The estimated mass is then used in the moment of inertia tensor estimator along with measurements from the manipulator's joint angles (θ_i) and corresponding angular velocities ($\dot{\theta}_i$), where the i represents the joint of the robotic arm ($i = 1, 2, 3$). Through an iterative process, the mass and moment of inertia tensor of the UAM are estimated at every instant in time during the UAM's maneuver.

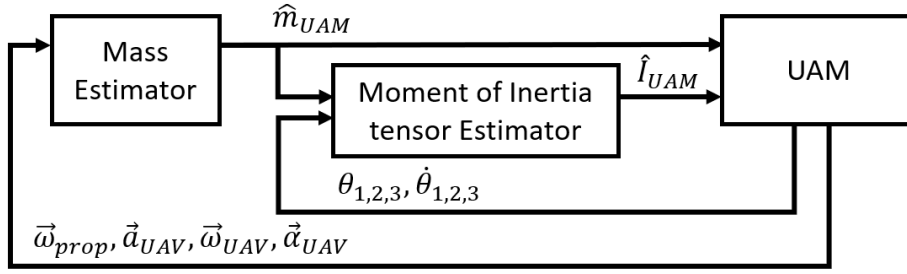


Fig. 2: The flowchart of inertia parameter estimators for a UAM.

3.1. Mass Estimator

The output of the mass estimator is the total mass of the UAM, m_{UAM} . As with traditional KF algorithms, the proposed approach employs two models: a motion model and a measurement model. The motion model for the UAM mass is set as a random walk model [16], represented by Eq. (1), where ε_m is defined as a Gaussian noise for the mass.

$$\dot{m}_{UAM} = \varepsilon_m \quad (1)$$

For the measurement model, the force of the UAM expressed in the UAV frame is used as given by Eq. (2). This model represents the relationship between the mass of the UAM and the forces acting on it.

$$\sum {}^{UAV}\vec{F}_{UAM} + m_{UAM} {}^{UAV}R_I \cdot \vec{g} = m_{UAM} {}^{UAV}\vec{a}_{UAM} \quad (2)$$

The term $\sum {}^{UAV}\vec{F}_{UAM}$ in Eq. (2) represents the forces acting on the center of mass of the UAM in the UAV frame of reference. The term ${}^{UAV}R_I$ is the rotational transformation matrix from the inertial reference frame to the UAV reference frame. The gravitational acceleration vector in the inertial reference frame is represented by \vec{g} , and ${}^{UAV}\vec{a}_{UAM}$ represents the acceleration of the UAM in the UAV reference frame. It is worth noting that ${}^{UAV}\vec{a}_{UAM}$ is difficult to measure directly since, in a typical UAV, an Inertia Measurement Unit (IMU) is fixed to the UAV and only provides the acceleration of the center of mass of the UAV but not the UAM. This is because, while the center of mass of the UAM continuously changes during any manipulation maneuvers, the center of mass of the UAV is fixed with respect to the UAV's frame of reference. Therefore, ${}^{UAV}\vec{a}_{UAM}$ in Eq. (2) is converted to the UAV's acceleration, ${}^{UAV}\vec{a}_{UAV}$, using the derivatives of the vector relation between the UAM and the UAV, ${}^{UAV}\vec{r}_{off}$ as illustrated in Fig. 3 and represented by Eq. (3).

$${}^{UAV}\vec{a}_{UAM} = {}^{UAV}\vec{a}_{UAV} + {}^{UAV}\ddot{\vec{r}}_{off} + {}^{UAV}\vec{\alpha}_{UAM} \times ({}^{UAV}\vec{r}_{off}) + 2 \cdot {}^{UAV}\vec{\omega}_{UAM} \times ({}^{UAV}\dot{\vec{r}}_{off}) + {}^{UAV}\vec{\omega}_{UAM} \times ({}^{UAV}\vec{\omega}_{UAM} \times ({}^{UAV}\vec{r}_{off})) \quad (3)$$

The term ${}^{UAV}\vec{r}_{off}$ in Eq. (3) represents the position vector of the center of mass of the UAM in the UAV frame. Assuming that the mechanical design and the kinematic motion of the robotic arm are fully known, it is reasonable to assume that the location of the center of mass of the UAM is known. Under this assumption, Eqs. (2) and (3) can be used to obtain Eq. (4).

$$\sum {}^{UAV}\vec{F}_{UAM} = m_{UAM} \left({}^{UAV}\vec{a}_{UAV} + {}^{UAV}\ddot{\vec{r}}_{off} + {}^{UAV}\vec{\alpha}_{UAM} \times ({}^{UAV}\vec{r}_{off}) + 2 \cdot {}^{UAV}\vec{\omega}_{UAM} \times ({}^{UAV}\dot{\vec{r}}_{off}) + {}^{UAV}\vec{\omega}_{UAM} \times ({}^{UAV}\vec{\omega}_{UAM} \times ({}^{UAV}\vec{r}_{off})) - {}^{UAV}R_I \cdot \vec{g} \right) \quad (4)$$

If the movement of the robotic arm is ignored, that is, assuming the arm is not moving during the time the estimation process is taking place, the center of mass of the UAM becomes static. Under such conditions, the UAM's angular velocity, $\vec{\omega}_{UAM}$, and angular acceleration, $\vec{\alpha}_{UAM}$, become equivalent to the UAV's angular velocity, $\vec{\omega}_{UAV}$, and the angular acceleration, $\vec{\alpha}_{UAV}$, which can be directly measured by the IMU on the UAV. Consequently, Eq. (4) can then be as Eq. (5), where ${}^{UAV}\vec{a}_{UAV}^P = {}^{UAV}\vec{a}_{UAV} - {}^{UAV}R_I \cdot \vec{g}$.

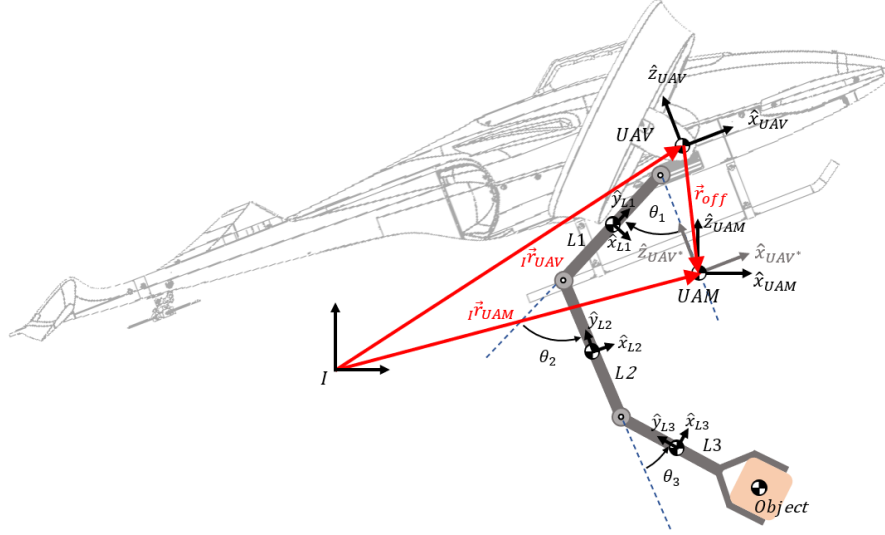


Fig. 3: Reference frames and vector relations.

$$\sum {}^{UAV}\vec{F}_{UAM} = m_{UAM} \left({}^{UAV}\vec{a}_{UAV}^P + {}^{UAV}\vec{\alpha}_{UAV} \times \left({}^{UAV}\vec{r}_{off} \right) + {}^{UAV}\vec{\omega}_{UAV} \times \left({}^{UAV}\vec{\omega}_{UAV} \times \left({}^{UAV}\vec{r}_{off} \right) \right) \right) \quad (5)$$

Thus, ${}^{UAV}\vec{a}_{UAV}^P$ can be directly measured by the accelerometers on the UAV. It should be noted that for this process to be effective, it is assumed that the UAM is not moving fast enough to be impacted by aerodynamic effects (e.g., drag force) during the mass estimation process. Therefore, the major forces acting on the UAM are the thrust forces from the UAV propellers (see Fig. 1-(c)). As a result, the term $\sum {}^{UAV}\vec{F}_{UAM}$ can be obtained by measuring the angular velocities of the propellers and combining them with the propellers' thrust coefficients [17], which are assumed to be known. The z-component of Eq. (5) can now be reformulated and a measurement noise (δ_m) is added to derive a measurement model, Eq. (6). To prevent Eq. (6) from diverging when the denominator becomes zero, which occurs when the aircraft is hovering, only the z-component of Eq. (5) is used.

$${}^{UAV}F_{UAM_z} \cdot \left\{ a_{UAV_z}^P + \dot{P}_{UAV}r_{off_y} - \dot{Q}_{UAV}r_{off_x} + P_{UAV} \left(R_{UAV}r_{off_x} - P_{UAV}r_{off_z} \right) - Q_{UAV} \left(Q_{UAV}r_{off_z} - R_{UAV}r_{off_y} \right) \right\}^{-1} = m_{UAM} + \delta_m \quad (6)$$

3.2. Moment of Inertia Tensor Estimator

After obtaining the estimation of the UAM's mass, the estimation of the UAM's inertia tensor can be obtained (Fig. 2). The parameters that need to be estimated are the moments of inertia (I_{xx} , I_{yy} , I_{zz}) and the product of inertia (I_{xz}) of the UAM, represented in a virtual frame of reference, UAV* (Fig. 3). This virtual UAV frame of reference is obtained by translating the UAV's frame of reference from its current position to the center of mass of the UAM. This

approach serves to ease the representation of the moments of inertia of the UAM with respect to the UAV. Since the given UAM is symmetric about its longitudinal plane (i.e., x-z plane) (Fig. 1-(c)), the products of inertia of the UAM in the x-y plane (I_{xy}) and the y-z plane (I_{yz}) are zero, which reduces the complexity in the estimation process.

To derive the motion and measurement model for the moment of inertia tensor estimation, the moment of inertia tensor of each component of the UAM and their derivatives in the UAV* frame are obtained using the rotated and parallel axis theorem [18] as Eq. (7).

$${}^{UAV^*}I_{c_i} = {}^{UAV^*}R_{c_i} \cdot c_i I_{c_i} \cdot {}^{UAV^*}R_{c_i}^T - m_{c_i} \cdot [{}^{UAV^*}\vec{r}_{c_i}]_{\times} \cdot [{}^{UAV^*}\vec{r}_{c_i}]_{\times} \quad (7)$$

In Eq. (7), the term $[]_{\times}$ refers to the skew-symmetric matrix, c_i represents one of the components comprising the given UAM. Herein, the components, c_i , comprising the UAM are the UAV, three arm linkages ($L1, L2, L3$), and the object being picked up (obj) (i.e., $c = [UAV, L1, L2, L3, obj]^T$). It is assumed that the object picked up by the manipulator is a point mass, and that it remains stationary once it has been picked up (i.e., a secure grasp is assumed). The time derivative of Eq. (7) is expressed as Eq. (8)

$$\begin{aligned} {}^{UAV^*}\dot{I}_{c_i} = & [{}^{UAV^*}\vec{\omega}_{c_i}]_{\times} \cdot {}^{UAV^*}R_{c_i} \cdot c_i I_{c_i} \cdot {}^{UAV^*}R_{c_i}^T - {}^{UAV^*}R_{c_i} \cdot c_i I_{c_i} \cdot {}^{UAV^*}R_{c_i}^T \cdot [{}^{UAV^*}\vec{\omega}_{c_i}]_{\times} \\ & + m_{c_i} \cdot 2 {}^{UAV^*}\vec{r}_{c_i} \cdot {}^{UAV^*}\vec{r}_{c_i} \cdot I^{3 \times 3} - {}^{UAV^*}\vec{r}_{c_i} \cdot {}^{UAV^*}\vec{r}_{c_i}^T - {}^{UAV^*}\vec{r}_{c_i} \cdot {}^{UAV^*}\vec{r}_{c_i}^T \end{aligned} \quad (8)$$

where ${}^{UAV^*}\vec{\omega}_{c_i}$ represents the angular velocity of c_i , which is measured and expressed with respect to the UAV* frame of reference. The moment of inertia tensor of the given UAM system and its derivative are then expressed as Eqs. (9) and (10), respectively.

$${}^{UAV^*}I_{UAM} = {}^{UAV^*}I_{UAV} + {}^{UAV^*}I_{L1} + {}^{UAV^*}I_{L2} + {}^{UAV^*}I_{L3} + {}^{UAV^*}I_{obj} \quad (9)$$

$${}^{UAV^*}\dot{I}_{UAM} = {}^{UAV^*}\dot{I}_{UAV} + {}^{UAV^*}\dot{I}_{L1} + {}^{UAV^*}\dot{I}_{L2} + {}^{UAV^*}\dot{I}_{L3} + {}^{UAV^*}\dot{I}_{obj} \quad (10)$$

As a result, the matrix components of Eq. (9) with additive gaussian noises (ε) serve as the measurement model, Eq. (11).

$$\begin{aligned} {}^{UAV^*}I_{UAM}(1,1) &= I_{xx} + \varepsilon_{xx} \\ {}^{UAV^*}I_{UAM}(2,2) &= I_{yy} + \varepsilon_{yy} \\ {}^{UAV^*}I_{UAM}(3,3) &= I_{zz} + \varepsilon_{zz} \\ {}^{UAV^*}I_{UAM}(3,1) &= I_{xz} + \varepsilon_{xz} \end{aligned} \quad (11)$$

Similarly, the matrix components of Eq. (10) with additive gaussian noises (δ) serve as the motion model, Eq. (12).

$$\begin{aligned} \dot{I}_{xx} &= {}^{UAV^*}\dot{I}_{UAM}(1,1) + \delta_{xx} \\ \dot{I}_{yy} &= {}^{UAV^*}\dot{I}_{UAM}(2,2) + \delta_{yy} \\ \dot{I}_{zz} &= {}^{UAV^*}\dot{I}_{UAM}(3,3) + \delta_{zz} \\ \dot{I}_{xz} &= {}^{UAV^*}\dot{I}_{UAM}(3,1) + \delta_{xz} \end{aligned} \quad (12)$$

By discretizing Eqs. (1), (6), (11) and (12), a KF mechanism can be used to estimate the mass and moment of inertia tensor of the UAM at all times.

4. Simulation Results

The proposed estimation mechanism has been validated in the MATLAB simulation environment by performing grasping tasks and flight motions using the Navig8 UAM (Fig. 1-(b)). Due to space constraints herein, a representative of results is presented which exemplifies the overall outcomes. For this, the mass and moment of inertia tensor of the components used during the simulations is summarized in Table. 1. It should be noted that the mass of the arm linkages assumed (i.e., In theory, it is not feasible for VTOL systems to lift more than one-third of their weight in real-life situations.) to test the proposed estimation filter under severe conditions. Furthermore, each of the three linkages comprising the arm is assumed to have the same inertia properties.

Table 1: Mass and moment of inertia of the UAM components.

	$m[kg]$	$I_{xx}[kg \cdot m^2]$	$I_{yy}[kg \cdot m^2]$	$I_{zz}[kg \cdot m^2]$	$I_{xz}[kg \cdot m^2]$
Navig8 UAV	5.0	0.0667	0.1492	0.2019	0.0147
Each arm linkage	1.0	0.0075	0.00001	0.0075	0.00001

During the simulation, the UAV is commanded to follow a set of sinusoidal roll (ϕ) and pitch (θ) motions, each having a different frequency and amplitude as shown in Fig. 4, while the robotic arm executes a pick-and-place operation of an unknown object. As illustrated in Fig. 5, the arm is initially positioned hanging from the UAV facing downward as the aircraft starts its motion ($t = 0$ s). Subsequently, at time $t=5$ s the arm is commanded to move forward for 5 seconds, after which it picks up a 2 kg object at $t = 10$ s. The arm is then commanded to move back to its initial position at time $t=15$ s (which executes in 5 seconds), and the object is released at 20 s.

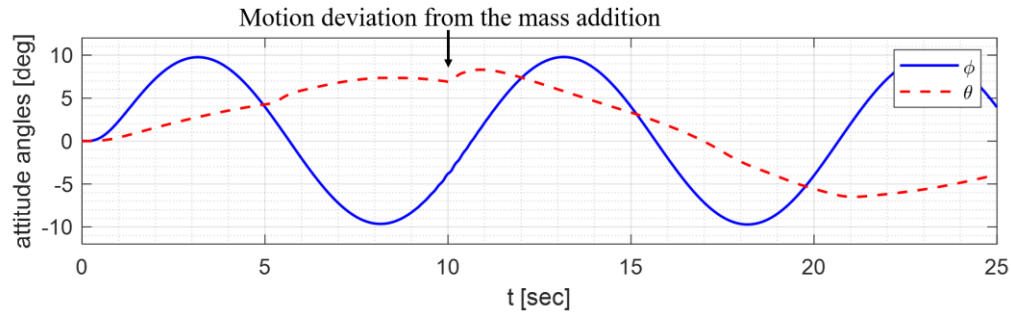


Fig. 4: Attitude angles of the UAV

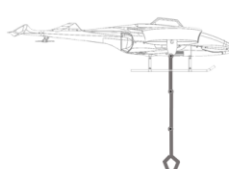
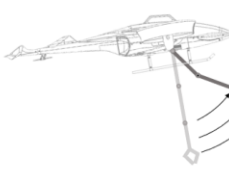
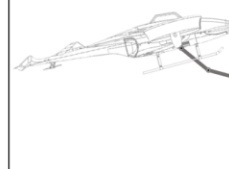
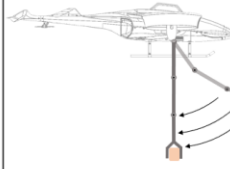
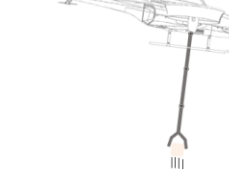
				
$\phi = 0 \text{ deg}$ $\theta = 0 \text{ deg}$	$\phi = -10 \sim 4 \text{ deg}$ $\theta = 4 \sim 7 \text{ deg}$	$\phi = -4 \text{ deg}$ $\theta = 7 \text{ deg}$	$\phi = -10 \sim 4 \text{ deg}$ $\theta = -6 \sim 3 \text{ deg}$	$\phi = -4 \text{ deg}$ $\theta = -6 \text{ deg}$
$\langle t = 0 \text{ s} \rangle$	$\langle t = 5 \sim 10 \text{ s} \rangle$	$\langle t = 10 \text{ s} \rangle$	$\langle t = 15 \sim 20 \text{ s} \rangle$	$\langle t = 20 \text{ s} \rangle$

Fig. 5: Time history of the arm and the UAV motion.

Additive Gaussian noise with a standard deviation of 20 rad/s is added to the measurement of the propellers' angular velocities. Additionally, the standard deviations of the noise added to the UAV's linear acceleration and angular velocity and acceleration measurements are defined to be 0.5 m/s^2 , 0.2 rad/s and 0.4 rad/s^2 , respectively. The

standard deviations of the measurement noises of the arm joints' angular positions and velocities are set to 0.08 rad and 0.2 rad/s , respectively. With these parameters, the proposed KF algorithm runs at 100 Hz .

Fig. 6 shows the estimated mass and moment of inertia tensor of the UAM during the entire duration of its task. The solid lines represent the estimated values, while the dashed lines indicate the corresponding true values. The top plot demonstrates that the total mass can be estimated within 1 second when mass variations exist (about 10 and 20 seconds). The rest of the plots show that the moment of inertia tensor can be tightly estimated when the manipulator is moving, and the estimated results converge to the true values within 1 second when the moment of inertia changes due to the added mass.

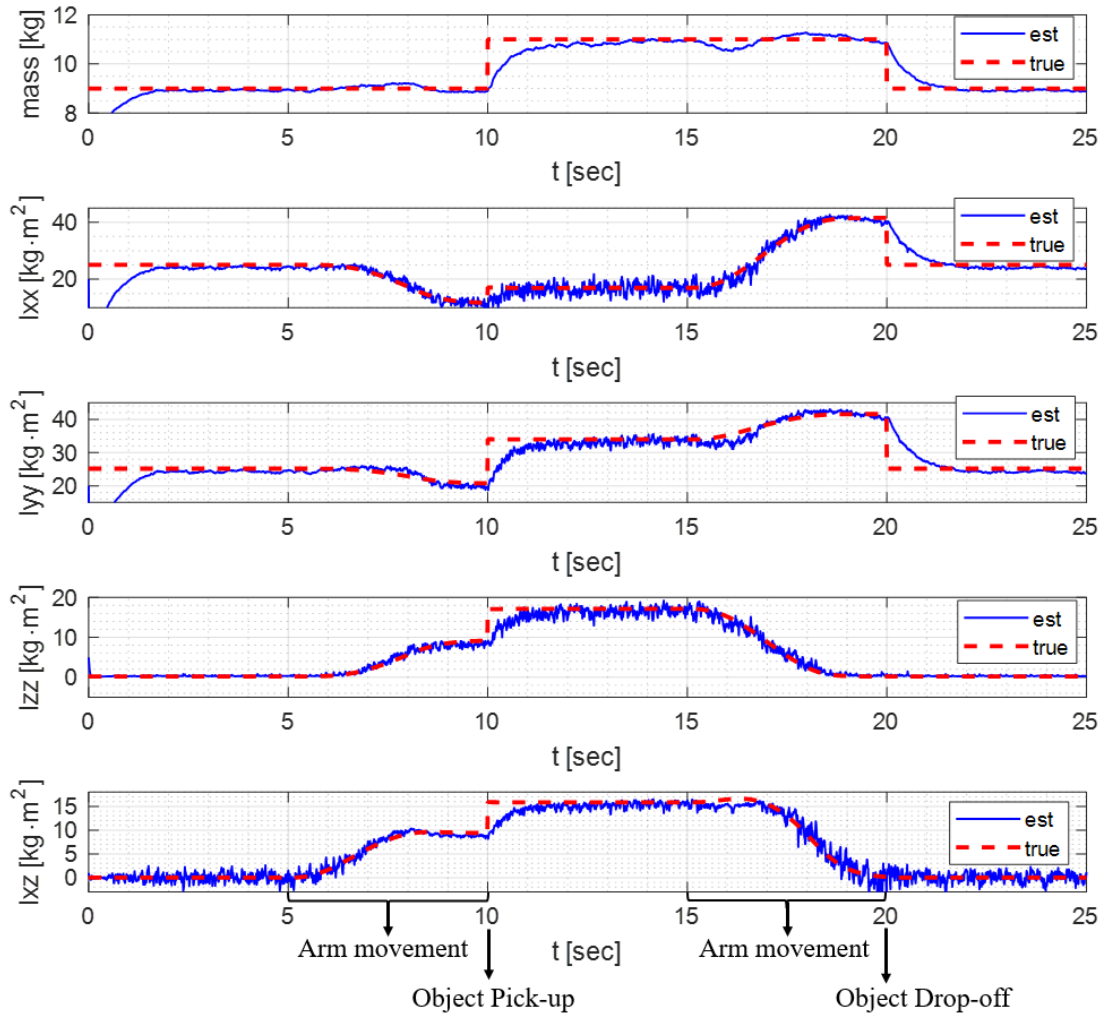


Fig. 6: Estimation results of the mass and the moment of inertia tensor and their corresponding true values.

5. Conclusions

In this paper, a method for estimating the varying mass and moment of inertia tensor of UAMs during manipulation maneuvers is presented. By considering both the dynamics of the UAM and the kinematics of the robotic arm, the mass and the moment of inertia tensor of the UAM are effectively estimated while the UAV performs flight maneuvers. The proposed method is validated through Matlab simulations, which result in tight estimations of varying inertia. Our future work will focus on developing estimation methods for the position of the center of mass of UAMs performing manipulation maneuvers.

References

- [1] F. Ruggiero, V. Lippiello, and A. Ollero, "Aerial manipulation: A literature review," *IEEE Robotics and Automation Letters*, vol. 3, no. 3, pp. 1957–1964, 2018.
- [2] A. Ollero, M. Tognon, A. Suarez, D. Lee, and A. Franchi, "Past, present, and future of aerial robotic manipulators," *IEEE Transactions on Robotics*, vol. 38, no. 1, pp. 626–645, 2021.
- [3] A. E. Jimenez-Cano, J. Martin, G. Heredia, A. Ollero, and R. Cano, "Control of an aerial robot with multi-link arm for assembly tasks," in *2013 IEEE International Conference on Robotics and Automation*. IEEE, 2013, pp. 4916–4921.
- [4] M. Orsag, C. Korpela, S. Bogdan, and P. Oh, "Dexterous aerial robots—mobile manipulation using unmanned aerial systems," *IEEE Transactions on Robotics*, vol. 33, no. 6, pp. 1453–1466, 2017.
- [5] C. Wang, B. Song, P. Huang, and C. Tang, "Trajectory tracking control for quadrotor robot subject to payload variation and wind gust disturbance," *Journal of Intelligent & Robotic Systems*, vol. 83, pp. 315–333, 2016.
- [6] T. N. Dief and S. Yoshida, "System identification and adaptive control of mass-varying quad-rotor," *Evergreen*, vol. 4, no. 1, pp. 58–66, 2017.
- [7] B. C. Min, J. H. Hong, and E. T. Matson, "Adaptive robust control (ARC) for an altitude control of a quadrotor type UAV carrying an unknown payloads," in *2011 11th International Conference on Control, Automation and Systems*. IEEE, 2011, pp. 1147–1151.
- [8] G. Baraban, M. Sheckells, S. Kim, and M. Kobilarov, "Adaptive parameter estimation for aerial manipulation," in *2020 American Control Conference (ACC)*. IEEE, 2020, pp. 614–619.
- [9] H. Lee, S. Kim, and H. J. Kim, "Control of an aerial manipulator using on-line parameter estimator for an unknown payload," in *2015 IEEE international conference on automation science and engineering (CASE)*. IEEE, 2015, pp. 316–321.
- [10] H. Lee and H. J. Kim, "Estimation, control, and planning for autonomous aerial transportation," *IEEE Transactions on Industrial Electronics*, vol. 64, no. 4, pp. 3369–3379, 2016.
- [11] D. Mellinger, Q. Lindsey, M. Shomin, and V. Kumar, "Design, modeling, estimation and control for aerial grasping and manipulation," in *2011 IEEE/RSJ International Conference on Intelligent Robots and Systems*. IEEE, 2011, pp. 2668–2673.
- [12] R. E. Kalman, "New results in linear filtering and prediction theory," *J. Basic Eng.*, vol. 83, no. 4, pp. 95–108, 1961.
- [13] P. Bagheri, A. Ramirez-Serrano, and J. K. Pieper, "Adaptive nonlinear robust control of a novel unconventional unmanned aerial vehicle," *Control and Intelligent Systems*, vol. 43, no. 1, pp. 274–280, 2015.
- [14] Majnoon, M., Samsami, K., Mehrandezh, M., and Ramirez-Serrano, A., "Dynamic Modeling and Vision-based Mobile target Tracking for a Rotary-wing UAV with Tilting Rotors", in *Canadian Society for Mechanical Engineering International Congress*, Kelowna, BC, Canada, June 26-29, 2016.
- [15] M. Yavari, K. Gupta, M. Mehrandezh, and A. Ramirez-Serrano, "Optimal real-time trajectory control of a pitch-hover uav with a two link manipulator," in *2018 International Conference on Unmanned Aircraft Systems (ICUAS)*. IEEE, 2018, pp. 930–938.
- [16] K. J. Keesman and K. J. Keesman, *System identification: an introduction*. Springer, 2011, vol. 2, pp. 175.
- [17] G. J. Leishman, *Principles of helicopter aerodynamics*. Cambridge university press, 2006, pp. 67.
- [18] R. N. Jazar, *Theory of applied robotics*. Springer, 2010, pp. 599.